

# Boundary Layer Approximation by Spectral/ $hp$ Methods

C. Schwab\*

M. Suri\*

C.A. Xenophontos\*

## Abstract

We present estimates for the approximation of boundary layer functions by spectral/ $hp$  type methods, both for the case that a *fixed* mesh (with one or more elements) or a *variable* mesh (with two elements) is used. We show that the best rate possible that is *uniform* with respect to the boundary layer parameter  $\varepsilon \in (0, 1]$  with a fixed mesh is  $O(p^{-1})$ , where  $p$  is the polynomial degree. For a variable mesh, we show that an *exponential* rate may be achieved, provided the first element is of size  $O(p\varepsilon)$ . We emphasize that no analytic or numerical matching of *outer* or *inner* asymptotic problems is required. We apply our results to a model singularly perturbed elliptic problem, as well as a one-dimensional advection-diffusion problem, obtaining exponential convergence estimates for each. Numerical results conform well with our theory. Although the results presented in this paper are one-dimensional, they can easily be extended to the treatment of boundary layers in higher-dimensional problems via (possibly mapped) tensor-product elements, even for unsmooth boundaries [14].

**Key words:** boundary layer, singularly perturbed problem,  $p$  version,  $hp$  version, spectral element method.

**AMS subject classifications:** 65N30, 35B30, 65N15.

## 1 Introduction

In this paper, we report on recent results in the approximation theory for *boundary layer functions*.

$$(1) \quad u(x) = \exp(-\lambda x/\varepsilon) \quad 0 < x < L,$$

where  $\varepsilon \in (0, 1]$  is a small parameter that can approach zero,  $\lambda = a + ib$  with  $a^2 + b^2 = 1$  and  $\operatorname{Re} a > 0$ . Here,

\*Department of Mathematics & Statistics, University of Maryland Baltimore County, Baltimore MD 21228-5398

ICOSAHOM'95: Proceedings of the Third International Conference on Spectral and High Order Methods. ©1996 Houston Journal of Mathematics, University of Houston.

$L \geq 1$  is a typical length scale of the problem under consideration. Previous approximation theory work along this line for the global error has led to optimal convergence estimates being established when a condition of the form  $N > C/\varepsilon^\alpha$  is satisfied (where  $N$  is the number of degrees of freedom used) — see, e.g, [9] for the  $h$  version FEM, [5] for spectral element methods, and [7] for spectral methods using “mapped” basis functions. Here, we are interested in obtaining convergence estimates that are *robust*, i.e. *uniform* in  $\varepsilon$ , when (1) is approximated by piecewise polynomials via  $p$  and  $hp$  type numerical schemes. Robust convergence estimates were obtained for  $h$ -versions of the finite element method in the one dimensional setting, for example, in [4, 13].

Let  $I = (c, d)$  be an open, bounded interval. By  $L^2(I)$  we denote the space of square integrable functions on  $I$ , equipped with the usual norm  $\|\cdot\|_0$ . For  $k \in \mathbb{N}$ , we denote by  $H^k(I)$  the Sobolev spaces of order  $k$  with norm  $\|\cdot\|_k$ . We set further  $H_0^1(I) = H^1(I) \cap \{u(c) = u(d) = 0\}$ .

## 2 The model problems

On  $I = (-1, 1)$ , consider the elliptic model problem

$$(2) \quad L_1 u = -\varepsilon^2 u'' + u = f$$

and the one-dimensional advection-diffusion problem

$$(3) \quad L_2 u = -\varepsilon u'' + u' = f$$

with the boundary conditions

$$(4) \quad u(-1) = u(1) = 0.$$

Here  $f \in L^2$  is a given function and  $0 < \varepsilon \leq 1$  is a small parameter (all function spaces are understood on  $I$ ).

### 2.1 Variational formulation

The weak formulation of (2), (4) is: Find  $u_1 \in H_0^1$  such that

$$(5) \quad B_1(u_1, v) = \int_{-1}^1 \{\varepsilon^2 u_1' v' + u_1 v\} dx = F(v)$$

for all  $v \in H_0^1$ .

For the problem (3), (4) we use a saddle-point formulation: Find  $u_2 \in L^2$  such that

$$(6) \quad B_2(u_2, v) = \int_{-1}^1 u_2 L_2^* v dx = F(v)$$

for all  $v \in H^2 \cap H_0^1$ .

Here  $F(v) = \int_I f v dx$  and  $L_2^* v = -\varepsilon v'' - v'$  is the formal adjoint to  $L_2$ .

On  $H_0^1$ , the bilinear form  $B_1(u, v)$  is coercive in the energy norm

$$(7) \quad \|u\|_\varepsilon = (B_1(u, u))^{1/2}.$$

Hence, for every  $f \in L^2$ , (5) admits a unique solution. The form  $B_2(u, v)$  is stable, i.e. there exists  $C > 0$  such that

$$(8) \quad \inf_{0 \neq u \in L^2} \sup_{0 \neq v \in H^2 \cap H_0^1} |B_2(u, v)| \geq C$$

(cf. [3]) so that (6) also admits a unique weak solution  $u_2 \in L^2$  for every  $f \in L^2$ .

### 2.2 Regularity

Generally, solutions of (2)–(4) exhibit *boundary layers*, i.e. solution components of the form

$$u_\varepsilon(x) = \exp(-(1+x)/\varepsilon), \quad \bar{u}_\varepsilon(x) = (-(1-x)/\varepsilon).$$

#### Theorem 2.1

Let  $f \in C^\infty(\bar{I})$ . Then for every  $M \in \mathbb{N}$ ,

$$(9) \quad u_1(x) = u_{asy}^M(x) + A^M u_\varepsilon(x) + B^M \bar{u}_\varepsilon(x)$$

where  $|A^M| + |B^M| + \|u_{asy}^M\|_\ell \leq C(M, f)$  for  $\ell = 0, 1, \dots, M$  with  $C(M, F)$  bounded independently of  $\varepsilon$ .

Similarly, for every  $M \in \mathbb{N}$ ,

$$(10) \quad u_2(x) = u_{asy}^M(x) + B^M(x) \bar{u}_\varepsilon(x)$$

where  $\|B^M\|_\ell + \|u_{asy}^M\|_\ell \leq C(M, f)$  for  $\ell = 0, 1, \dots, M$  with  $C(M, F)$  bounded independently of  $\varepsilon$ .

The proof is standard and can be found in [6, Theorem 2.2] and [11, Theorem 2.1]. The parameter  $\varepsilon$  is the length scale of the boundary layers. We observe that  $u_1(x)$  has, in general, layers at both ends of  $I$  whereas  $u_2(x)$  has only one layer at the “outflow” boundary  $x = 1$ .

We note that  $u_\varepsilon(x)$  and  $\bar{u}_\varepsilon(x)$  are of the form (1) with  $\lambda = a + ib = 1$ . The case where  $b \neq 0$  will be also contained in our approximation results in Section 4 ahead, since it arises, for example, for elliptic shells, where  $a = b = 1/\sqrt{2}$  and  $\varepsilon = \sqrt{t}$  in the layer stemming from the simple edge effect (see, e.g., [8]) with  $t$  denoting the shell thickness.

## 3 The finite element methods

We obtain approximate solutions by restricting the variational formulations (5), (6) to finite-dimensional subspaces.

By  $\Delta = \{-1 = x_0 < x_1 < x_2 < \dots < x_m = 1\}$  we denote a mesh in  $[-1, 1]$  and set  $I_j = (x_{j-1}, x_j)$ ,  $h_j = x_j - x_{j-1}$  for  $j = 1, \dots, m$ . We let further  $\vec{p} = (p(1), \dots, p(m))$ ,  $p(j) \geq 1$ , denote a polynomial degree vector. Then we define

$$(11) \quad \tilde{S}^{\vec{p}}(\Delta) = \left\{ u \in C^0(I) : u|_{I_j} \in \Pi_{p(j)}(I_j), \right. \\ \left. j = 1, \dots, m \right\}.$$

$$(12) \quad S^{\vec{p}}(\Delta) = \tilde{S}^{\vec{p}}(\Delta) \cap \{u | u(\pm 1) = 0\}$$

Here,  $\Pi_p(I)$  denotes polynomials of degree  $\leq p$ .

Evidently,  $S^{\vec{p}}(\Delta) \subset H_0^1$ . The discretization of (5) is: Find  $u_1^{FE} \in S^{\vec{p}}(\Delta)$  such that

$$(13) \quad B_1(u_1^{FE}, v) = F(v) \quad \forall v \in S^{\vec{p}}(\Delta)$$

which, for every  $\varepsilon > 0$ , admits a unique solution.

To obtain a stable discretization of (6) we use again  $S^{\vec{p}}(\Delta)$  as a trial space. Since  $H^2$ -conforming test function spaces are difficult to construct, (6) is reformulated on spaces with mesh-dependent norms.

Let  $H_\Delta^0$  denote the completion of  $H_0^1$  with respect to the norm

$$\|u\|_{H_\Delta^0} = \left( \|u\|_0 + \sum_{j=1}^{m-1} \rho_j |u(x_j)|^2 \right)^{1/2}$$

where  $\rho_j := (h_j + h_{j+1})/2$ ,  $j = 1, \dots, m-1$ . Then  $H_\Delta^0$  is isomorphic to  $L^2 \oplus \mathbb{R}^{m-1}$ , i.e.

$$u = (\tilde{u}, d_1, \dots, d_{m-1}) \in H_\Delta^0 = L^2 \oplus \mathbb{R}^{m-1}$$

and

$$(14) \quad \|u\|_{H_\Delta^0} = \left( \|\tilde{u}\|_0 + \sum_{j=1}^{m-1} \rho_j |d_j|^2 \right)^{1/2}.$$

If  $u \in H_\Delta^0 \cap H^1$ , then  $\tilde{u} = u$  and  $d_j = u(x_j)$ . As test space we introduce

$$(15) \quad H_\Delta^2 = H_0^1 \cap \left\{ v : v|_{I_j} \in H^2(I_j) \right\}$$

equipped with the norm

$$\|u\|_{H_{\varepsilon, \Delta}^2} = \left\{ \sum_{j=1}^m \int_{I_j} |L_2^* v|^2 dx + \sum_{j=1}^{m-1} \frac{|\varepsilon \mathcal{J}(v'(x_j))|^2}{\rho_j} \right\}^{1/2}$$

where

$$\mathcal{J}(v'(x_j)) = v'(x_j + 0) - v'(x_j - 0)$$

is the jump of  $v'$  at  $x_j$ . Note that  $H_0^1 \subset H_\Delta^0 \subset L^2$  and  $H_0^1 \supset H_\Delta^2 \supset H^2 \cap H_0^1$ . On  $H_\Delta^0 \times H_\Delta^2$  we define a bilinear form  $B_\Delta(\cdot, \cdot)$  by

$$(16) \quad B_\Delta(u, v) = \sum_{j=1}^m \int_{I_j} \tilde{u} L_2^* v dx - \sum_{j=1}^{m-1} \varepsilon d_j \mathcal{J}(v'(x_j)).$$

Clearly,  $B_\Delta$  restricted to  $H_\Delta^0 \times (H^2 \cap H_0^1)$  coincides with  $B_2$ , i.e.  $B_\Delta$  is an extension of  $B_2(\cdot, \cdot)$ .

The weak form of (3), (4) to be discretized reads: Find  $u_2 \in H_\Delta^0$  such that

$$(17) \quad B_\Delta(u_2, v) = F(v) \quad \forall v \in H_\Delta^2.$$

We have for every mesh  $\Delta$  [3]:

$$\inf_{0 \neq u \in H_\Delta^0} \sup_{0 \neq v \in H_\Delta^2} |B_\Delta(u, v)| \geq \|u\|_{H_\Delta^0} \|v\|_{H_{\varepsilon, \Delta}^2}$$

$$\forall 0 \neq u \in H_\Delta^0 : \sup_{0 \neq v \in H_\Delta^2} B_\Delta(u, v) > 0$$

so that (17) has a unique solution  $u_2$  for every  $f \in L^2$ . A conforming discretization of (17) is obtained with the  $L$ -spline test space

$$(18) \quad S_{L_2}^{\bar{p}}(\Delta) = \left\{ v \in C^0(I) : (L_2^* v)|_{I_j} = 0 \text{ if } p(j) = 1, \right. \\ \left. (L_2^* v)|_{I_j} \in \Pi_{p(j)-2}(I_j) \text{ if } p(j) \geq 2, \right. \\ \left. v(\pm 1) = 0 \right\}.$$

Then the discrete form of (17) is: Find  $u_2^{FE} \in S^{\bar{p}}(\Delta)$  such that

$$(19) \quad B_\Delta(u_2^{FE}, v) = F(v) \quad \forall v \in S_{L_2}^{\bar{p}}(\Delta).$$

We can prove the following spectral stability result [14].

**Theorem 3.1** For every  $\Delta$

$$\inf_{u \in S^{\bar{p}}(\Delta)} \sup_{v \in S_{L_2}^{\bar{p}}(\Delta)} |B_\Delta(u, v)| \geq C_s \|u\|_{H_\Delta^0} \|v\|_{H_{\varepsilon, \Delta}^2}$$

with the stability constant given by

$$C_s^2(p, \Delta) = \frac{1}{1 + p \max_{1 \leq j \leq m-1} \{\rho_j\}}$$

where  $p = \max_{1 \leq j \leq m} \{p(j)\}$ .

For every  $\bar{p}$  and  $\Delta$  there exists a unique solution of (19).

Moreover, the finite element solutions  $u_i^{FE}$  are quasi-optimal, i.e.

$$(20) \quad \|u_1 - u_1^{FE}\|_\varepsilon \leq \|u_1 - v\|_\varepsilon$$

and

$$(21) \quad \|u_2 - u_2^{FE}\|_{H_\Delta^0} \leq (1 + C/C_s(p, \Delta)) \|u_2 - v\|_{H_\Delta^0}$$

for every  $v \in S^{\bar{p}}(\Delta)$ .

## 4 The $p$ and $hp$ boundary layer approximation

We analyze the approximation of boundary layer functions of the type (1), along the lines of [11]. We give proofs of the error estimates which are simpler and shorter compared to those in [11], but do not explicitly yield the values of constants, and cannot be used to establish pre-asymptotic error estimates. Nevertheless, these are sufficient to establish uniform (in  $a$ ) exponential convergence as the spectral order  $p$  tends to  $\infty$ . In the case of complex  $\lambda$ , however, they generalize the results of [11].

We begin with a basic approximation result on a single element.

**Theorem 4.1** Let  $u_{\lambda, \varepsilon}(x) = \exp(-\lambda(x+1)/\varepsilon)$ ,  $x \in (-1, 1)$  with  $\varepsilon > 0$ ,  $\lambda = a + ib$ ,  $a^2 + b^2 = 1$ . Then, for every  $p \geq 1$ , there exists  $s_p \in \Pi_p(I)$  such that

$$(22) \quad s_p(\pm 1) = u_{\lambda, \varepsilon}(\pm 1),$$

$$(23) \quad \|u'_{\lambda, \varepsilon} - s'_p\|_{L_2(I)}^2 \leq C\varepsilon^{-1} \left( \frac{e}{(2p+1)\varepsilon} \right)^{2p+1},$$

$$(24) \quad \|u_{\lambda, \varepsilon} - s_p\|_{L_2(I)}^2 \leq C\varepsilon p^{-1} \left( \frac{e}{(2p+1)\varepsilon} \right)^{2p+1}.$$

**Proof** It follows from Thm. 3.3.4 of [2] that there exists  $s_p \in \Pi_p(I)$  satisfying (22), and such that

$$(25) \quad \|u'_{\lambda, \varepsilon} - s'_p\|_{L_2(I)}^2 \leq \frac{1}{(2p)!} |u'_{\lambda, \varepsilon}|_{V^p(I)}^2$$

and

$$(26) \quad \|u_{\lambda, \varepsilon} - s_p\|_{L_2(I)}^2 \leq \frac{1}{p(p+1)(2p-1)!} |u'_{\lambda, \varepsilon}|_{V^{p-1}(I)}^2$$

where

$$|u'|_{V^q(I)}^2 := \int_{-1}^1 (1 - \xi^2)^q |u^{(q+1)}(x)|^2 dx.$$

Now,

$$\begin{aligned} |u_{\lambda, \varepsilon}^{(q+1)}(x)|^2 &= \varepsilon^{-2(q+1)} |\lambda|^{2(q+1)} |\exp(-\lambda(x+1)/\varepsilon)|^2 \\ &= \varepsilon^{-2(q+1)} e^{-2a(x+1)/\varepsilon} \end{aligned}$$

since  $|\lambda| = 1$ . Hence,

$$\begin{aligned} |u'_{\lambda, \varepsilon}|_{V^q(I)}^2 &= \varepsilon^{-2(q+1)} \int_{-1}^1 (1 - \xi^2)^q e^{-2a(\xi+1)/\varepsilon} d\xi \\ (27) \quad &\leq \varepsilon^{-2(q+1)} \int_{-1}^1 (1 - \xi^2)^q d\xi \\ &\leq C\varepsilon^{-2(q+1)} (q+1)^{-1/2}. \end{aligned}$$

Stirling's formula yields

$$(28) \quad \frac{1}{(2q)!} \leq C \left( \frac{e}{2q+1} \right)^{2q+1/2}$$

where  $C$  is independent of  $q$ . Combining (25)-(28), we get (23) and (24).  $\square$

Estimates (23) and (24) imply super-exponential convergence as  $p \rightarrow \infty$ , provided

$$(29) \quad \tilde{p} := p + \frac{1}{2} > e/2\varepsilon.$$

For small values of  $\varepsilon$ , (29) will only be satisfied for unrealistically high values of  $p$ . In fact, it is shown in [11] that when  $p$  is not of the order given by (29), the super-exponential convergence deteriorates. Using more refined techniques of proof for Theorem 4.1 (see [11]), which involve Bessel functions, we may derive pre-asymptotic estimates for the range where  $\tilde{p}$  does not satisfy (29). With such estimates, it may be shown [11] that the best rate uniform in  $\varepsilon$  that may be obtained by the  $p$  or spectral version on a fixed mesh is essentially  $O(p^{-1})$ .

**Theorem 4.2** *Let  $u_{\lambda,\varepsilon}$  be as in Theorem 4.1. Let  $\tilde{S}^{\tilde{p}}(\Delta)$  correspond to the pure  $p$  version (or spectral element method) on a fixed mesh  $\Delta$ . Then*

$$\frac{C}{p} \leq \sup_{\varepsilon \in (0,1]} \inf_{\substack{v \in \tilde{S}^{\tilde{p}}(\Delta) \\ v(\pm 1) = u_{\lambda,\varepsilon}(\pm 1)}} \|u_{\lambda,\varepsilon} - v\|_\varepsilon \leq \frac{C}{p} \sqrt{\ln p},$$

where the constant  $C$  is independent of  $\varepsilon$  and  $p$ .

We now consider an  $hp$  approximation result, where the mesh changes at each step that  $p$  is increased. It turns out that only the relative size, and not the number of elements needs to be altered to already achieve exponential convergence (more precisely, this is an “ $rp$ ” version).

**Theorem 4.3** *Let  $u_{\lambda,\varepsilon}$  be as in Theorem 4.1. Let,  $(\Delta, \tilde{p})$  be such that for some  $\kappa$  independent of  $p, \varepsilon$  satisfying  $0 < \kappa_0 \leq \kappa < 4/e$ ,*

$$\begin{aligned} \tilde{p} = \{p, 1\}, \quad \Delta = \{-1, -1 + \kappa\tilde{p}\varepsilon, 1\} & \text{ if } \kappa\tilde{p}\varepsilon < 2 \\ \tilde{p} = \{p\}, \quad \Delta = \{-1, 1\} & \text{ if } \kappa\tilde{p}\varepsilon \geq 2. \end{aligned}$$

Then there exists  $u_p \in \tilde{S}^{\tilde{p}}(\Delta)$  satisfying  $u_p(\pm 1) = u_{\lambda,\varepsilon}(\pm 1)$  and

$$(30) \quad \|u_{\lambda,\varepsilon} - u_p\|_\varepsilon \leq C\varepsilon^{1/2}q^{\tilde{p}},$$

$$(31) \quad \|u_{\lambda,\varepsilon} - u_p\|_0 \leq C\varepsilon^{1/2}q^{\tilde{p}},$$

$$(32) \quad \|u_{\lambda,\varepsilon} - u_p\|_1 \leq C\varepsilon^{-1/2}q^{\tilde{p}}.$$

Here, the constants are independent of  $p$  and  $\varepsilon$  but depend on  $\kappa_0$  and  $q < 1$  is given by

$$(33) \quad q := \begin{cases} e/2\tilde{p}\varepsilon & \text{if } \kappa\tilde{p}\varepsilon \geq 2 \\ \max\{\kappa e/4, e^{-a(\kappa-\delta)}\} & \text{otherwise} \end{cases}$$

with  $\delta > \ln \tilde{p}/2\tilde{p}$  arbitrary.

**Proof** If  $\kappa\tilde{p}\varepsilon \geq 2$ , then we obtain the result directly from Theorem 4.1, since  $\kappa < 4/e$  implies  $q = e/(2\tilde{p}\varepsilon) < 1$ .

Suppose  $\kappa\tilde{p}\varepsilon < 2$ . We then construct the function  $u_p(x)$  element-wise. Let  $c = -1 + \kappa\tilde{p}\varepsilon$  and  $I_1 = (-1, c)$ . Transforming  $I_1$  to  $I = (-1, 1)$ , we see that for  $t = 0, 1$ ,

$$(34) \quad \int_{-1}^c \left( \frac{dt f}{dx^t} \right)^2 dx = \left( \frac{2}{\kappa\tilde{p}\varepsilon} \right)^{2t-1} \int_{-1}^1 \left( \frac{dt \tilde{f}}{dy^t} \right)^2 dy.$$

Here,  $\tilde{f}(y)$  denotes the image on  $I$  of any function  $f(x)$  defined on  $I_1$ . In particular, for  $\tilde{\varepsilon} = 2/\kappa\tilde{p}$  we have

$$(35) \quad \tilde{u}_{\lambda,\varepsilon}(y) = \exp(-\lambda(y+1)\kappa\tilde{p}/2) = u_{\lambda,\tilde{\varepsilon}}(y).$$

We apply Theorem 4.1 to  $u_{\lambda,\tilde{\varepsilon}}(y)$ . Transforming back, we obtain a polynomial  $s_p \in \Pi_p(I_1)$  such that

$$(36) \quad s_p(-1) = u_{\lambda,\varepsilon}(-1), \quad s_p(c) = u_{\lambda,\varepsilon}(c),$$

$$(37) \quad \begin{aligned} & \| (u_{\lambda,\varepsilon} - s_p)' \|_{L_2(I_1)}^2 \\ & \leq C\varepsilon^{-1} \left( \frac{e}{\tilde{p}\tilde{\varepsilon}} \right)^{2p+1} \left( \frac{2}{\kappa\tilde{p}\varepsilon} \right) \\ & = C\varepsilon^{-1} \left( \frac{e\kappa}{4} \right)^{2p+1} \leq C\varepsilon^{-1}q^{2\tilde{p}} \end{aligned}$$

and

$$(38) \quad \begin{aligned} & \| (u_{\lambda,\varepsilon} - s_p) \|_{L_2(I_1)}^2 \\ & \leq C\varepsilon p^{-1} \left( \frac{e}{\tilde{p}\tilde{\varepsilon}} \right)^{2p+1} \left( \frac{2}{\kappa\tilde{p}\varepsilon} \right)^{-1} \\ & = C\varepsilon p^{-1} \left( \frac{e\kappa}{4} \right)^{2p+1} \leq C\varepsilon q^{2\tilde{p}}. \end{aligned}$$

It is seen by (37), (38) that the error in this first interval  $I_1$  satisfies (30)-(32).

For simplicity, we will only demonstrate that  $u_p$  may be defined on the second interval so as to satisfy the end conditions and the estimate (32). To obtain a function simultaneously satisfying the  $L^2$  estimate (31) as well, some technical changes have to be made in the definition of  $u_p$ , the details of which may be found in [11].

First, we note that

$$|u_{\lambda,\varepsilon}(c)| \leq e^{-\alpha\kappa\bar{p}}.$$

Then we define  $u_p(x)$  to be the linear interpolant of  $u_{\lambda,\varepsilon}$  at  $x = c$  and  $x = 1$  to get

$$\|u'_p\|_{L_2(I_2)} \leq C e^{-\alpha\kappa\bar{p}}$$

uniformly in  $\varepsilon, c$  for  $c < 1$ . Using the triangle inequality, it follows that

$$(39) \quad \|u'_{\lambda,\varepsilon} - u'_p\|_{L_2(I_2)} \leq \|u'_{\lambda,\varepsilon}\|_{L_2(I_2)} + \|u'_p\|_{L_2(I_2)} \\ \leq C\varepsilon^{-1/2} e^{-\alpha\kappa\bar{p}}.$$

Then (32) follows from (37), (39).  $\square$

The following corollary follows immediately from Theorem 4.3, by using the interpolation inequality

$$\|u\|_{L^\infty(I)} \leq 2\|u\|_0^{1/2} \|u'\|_0^{1/2}.$$

**Corollary 4.1** *Let  $u_{\lambda,\varepsilon}, u_p$  be as in Theorem 4.3. Then*

$$\|u_{\lambda,\varepsilon} - u\|_{L^\infty} \leq Cq^{\bar{p}}$$

where  $q$  is as in (33) and  $C$  is a constant independent of  $p, \varepsilon$ .

These approximation results imply exponential convergence, uniform in  $\varepsilon$ , of the finite element methods (13), (19). To illustrate this for (19), consider the problem (17) with  $f(x) = -1/2$  and exact solution

$$u_2(x) = \frac{\exp((x+1)/\varepsilon) - 1}{\exp(2/\varepsilon) - 1} - \frac{x+1}{2}.$$

The solution consists of a smooth (polynomial) part and a boundary layer at  $x = 1$ , as expected from Theorem 2.1. Further, from the definition of  $\|u\|_{H_\Delta^0}$  it is easy to see that

$$(40) \quad \|u - v\|_{H_\Delta^0}^2 \leq \|u - v\|_0^2 + 2\|u - v\|_{L^\infty}^2.$$

Since the linear part is contained in  $S^{\bar{p}}(\Delta)$ , the finite element error is essentially the boundary layer approximation error. Hence, using the two-element mesh from Theorem 4.3, we find with (21) and (40) the error estimate

$$\|u_2 - u_2^{FE}\|_{H_\Delta^0} \leq C\sqrt{pq}^{\bar{p}}$$

i.e. a robust exponential convergence rate.

## 5 Numerical results

We present the results of numerical computations for the model problem (5) where

$$f(x) = -\frac{x+1}{2}.$$

This problem was also considered in [5, 7] and its exact solution is

$$(41) \quad u_1(x) = \frac{\sinh((x+1)/\varepsilon)}{\sinh(2/\varepsilon)} - \frac{x+1}{2}.$$

Evidently, it has only one boundary layer near  $x = 1$ , i.e.  $A_M = 0$  in (9). Since we have, moreover,

$$(42) \quad \|u_1\|_\varepsilon^2 = B_1(u_1, u_1) = (1, u_1) = O(1)$$

we conclude that the relative error in the energy norm,

$$E_R(d) = \|u_1 - u_1^{FE}\|_\varepsilon / \|u_1\|_\varepsilon$$

should behave like  $\Phi(\varepsilon, S^{\bar{p}}(\Delta))$  where

$$(43) \quad \Phi(\varepsilon, S) := \inf_{\chi \in S} \|u_1 - \chi\|_\varepsilon.$$

Since  $u_{asy}^M(x) \in \Pi_1(-1, 1)$  for  $M \geq 1$ , the asymptotic behavior of the error is completely governed by the boundary layer approximation error for  $S^{\bar{p}}(\Delta)$ . Since, moreover,  $u_1$  in (41) has only one boundary layer near  $x = 1$ , i.e.  $A_M = 0$  in (9), Theorem 4.3 requires  $S^{\bar{p}}(\Delta)$  with

$$(44) \quad \Delta = \{-1, 1 - \kappa\bar{p}\varepsilon, 1\}, \quad \bar{p} = (1, p).$$

Evidently,  $N = \dim S^{\bar{p}}(\Delta) = p + 1$  then.

We will now depict  $E_R(d)$  versus the number of degrees of freedom in the finite element method. We compare four finite element methods: (a) the  $p$  version with one element, (b) the  $h$  version with  $p = 1$ , (c) the  $hp$  version with 2 elements with  $S^{\bar{p}}(\Delta)$  as in (44) and  $\kappa = 1$  and (d) the  $h$  version (taking  $p = 1$ ) with the exponential mesh  $\Delta = \{-1, x_1, \dots, x_{m-1}, 1\}$  where, for  $m$  even,

$$(45) \quad x_i = \begin{cases} -1 & \text{if } i = 0, \\ -d\bar{p} \ln\left(1 - c\frac{i-1}{m-1}\right), & i = 1, \dots, m. \end{cases}$$

and  $c = 1 - \exp(-1/(d\bar{p}))$ . The mesh (45) is derived in [12], [14], where it is shown that when the  $h$  version is used with  $p = 1$ , the error obtained with this mesh is asymptotically optimal as  $m \rightarrow \infty$ . All computations were done in double precision on an SGI-2 workstation using MATLAB 4.2a.

Figures 1, 2 and 3 show the performance of the four methods for  $\varepsilon = 10^{-2}, \varepsilon = 10^{-4}$  and  $\varepsilon = 10^{-8}$ , respectively. (We obtained graphs analogous to these figures for

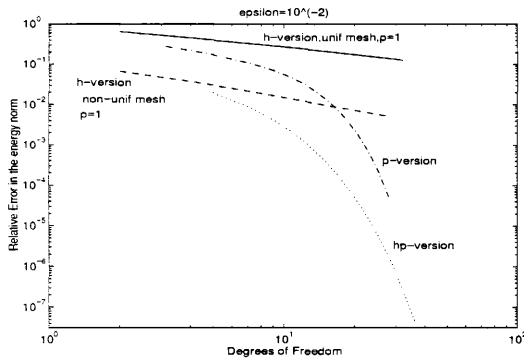


Figure 1: Comparison of various methods.

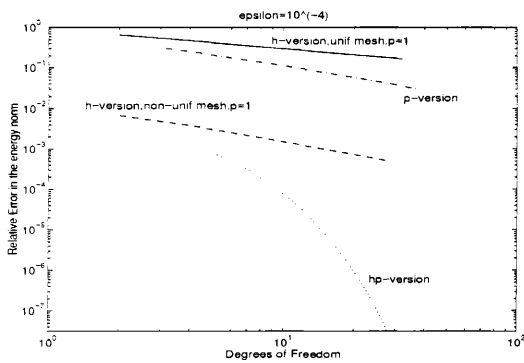


Figure 2: Comparison of various methods.

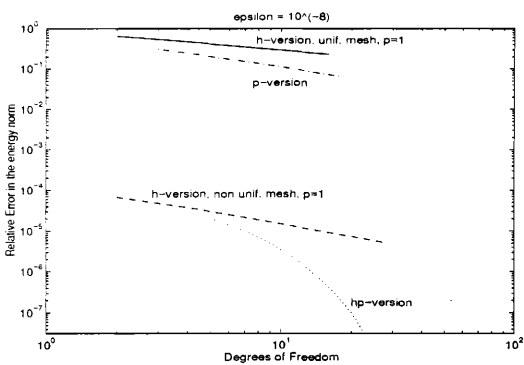


Figure 3: Comparison of various methods.

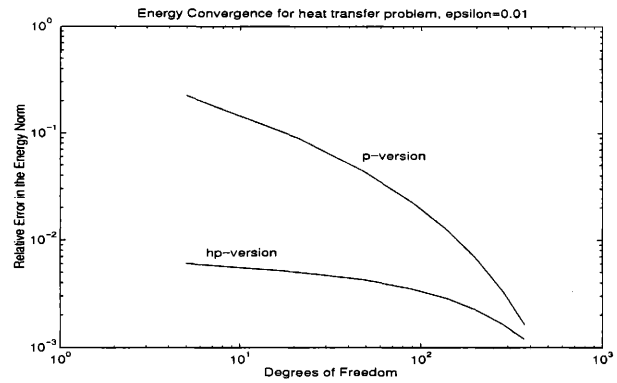


Figure 4:  $p$  and  $hp$  energy convergence for (5.6),  $\varepsilon = 0.01$ .

$\varepsilon$  ranging from  $10^{-1}$  to  $10^{-8}$ .) To illustrate that our one-dimensional results are, via tensor product arguments, also applicable to two- and three-dimensional singularly perturbed problems, we consider the following model heat transfer problem, the two-dimensional analog of (2). For a detailed analysis, we refer to [14]. In the unit circle  $\Omega = \{(r, \theta) : 0 \leq \theta \leq 2\pi, 0 \leq r \leq 1\}$  we consider

$$(46) \quad \begin{aligned} -\varepsilon^2 \Delta u + u &= 1 \text{ in } \Omega, \\ u &= 0 \text{ on } \partial\Omega. \end{aligned}$$

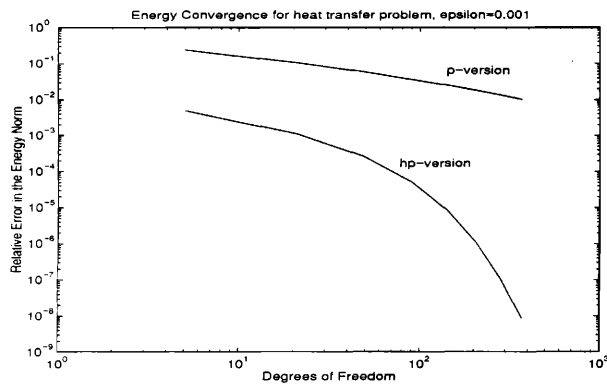
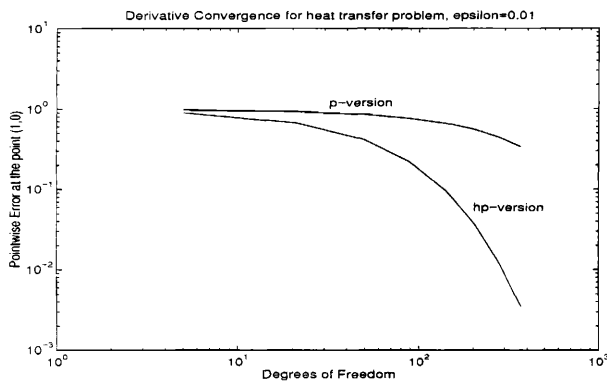
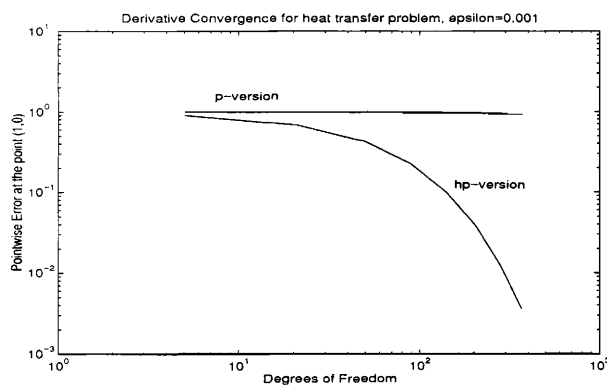
The exact solution is given by

$$u(r, \theta) \equiv u(r) = 1 - \frac{I_0(r/\varepsilon)}{I_0(1/\varepsilon)},$$

where  $I_0(x)$  is the modified Bessel function of order zero. We performed numerical experiments for this model problem using the finite element package STRESSCHECK<sup>TM</sup>, for the  $p$  and  $hp$  versions, with equal number of degrees of freedom. The error plots in Figures 4 and 5 show once more the convergence in the energy norm. The boundary layer mesh also gives accurate pointwise function- and derivative values. To illustrate this, we show in Figures 6 and 7 the pointwise convergence of the normal derivative on the perimeter of the circle  $\Omega$ .

Let us summarize some of the observations that can be made from the above figures.

- (1) The rate of convergence of the uniform  $h$  version is  $O(N^{-1/2})$  while the uniform (in  $\varepsilon$ ) rate for the  $p$  version on a single element is  $O(N^{-1})$ , which is *double* the  $h$  version rate. For the  $h$  version with exponential mesh, the optimal algebraic rate of  $O(N^{-1})$  is observed, while the  $hp$  version shows *exponential* rate, and outperforms all the other methods.

Figure 5:  $p$  and  $hp$  energy convergence for (5.6),  $\varepsilon = 0.001$ .Figure 6: Normal derivative error at  $(1, 0)$ ,  $\varepsilon = 0.01$ .Figure 7: Normal derivative error at  $(1, 0)$ ,  $\varepsilon = 0.001$ .

- (2) The errors for the  $h$  version with exponential mesh and the  $hp$  version both *decrease* as  $\varepsilon$  becomes smaller, at the rate of  $O(\varepsilon^{1/2})$ . The other two versions do not display this decrease as  $\varepsilon \rightarrow 0$ .
- (3) Asymptotically, the  $p$  version with a single element will always have the best convergence rate for any fixed  $\varepsilon$  according to Theorem 4.1. However, as seen from Figures 1 - 3, in practice this asymptotic convergence is not usually observed. In Figure 1, the slope of the error curve for the largest  $p$  is better than the one for the 2 element  $hp$  version, showing that at this point, the  $p$  version is decreasing at a fast rate. However,  $E_R(d)$  for the  $p$  version is still several orders of magnitude larger than the value for the 2-element  $hp$  version.
- (5) For a fixed number of degrees of freedom, the error with the  $hp$  version is seen to be consistently the smallest of the four methods. This version is extremely robust and efficient — even for very small values of  $\varepsilon$ , relative energy errors of  $10^{-8}$  were reached with only  $N = 15$  degrees of freedom.
- (5) Although we report here only the relative energy error, the *pointwise error* was found to behave completely analogously (as could be expected by Corollary 4.1).
- (6) Our results with the  $hp$  method compare very favorably with the numerical results presented in [7] for the same problem, in which a significant improvement over the pure spectral element was achieved by using special “mapped” polynomials.

## 6 Conclusion

We analyzed spectral element/ $hp$  finite element discretizations for two one-dimensional, singularly perturbed model problems, the solutions of which behave like a smooth (analytic) function in the interior of the interval but have boundary layers at one or both end points. For problem (5), a symmetric selection of test and trial spaces leads trivially to a stable method. For the advection diffusion problem, the saddle point formulation (17) going back to [3] is discretized. Selecting the  $L_2$ -spline test function space (18) ensures stability (in the sense of Theorem 3.1) if  $p \rightarrow \infty$ . We showed theoretically that using a  $p$  version FEM or spectral element method on a *fixed* mesh, the best possible robust rate uniform in  $\varepsilon$  cannot exceed  $O(p^{-1})$ . We also showed that an  $hp$  version FEM or spectral element method with one “boundary layer element” of width  $O(\varepsilon p)$  achieves robust (in  $\varepsilon$ ) exponential convergence rates, for

both the elliptic-elliptic and advection diffusion problem. In numerical experiments, our method consistently outperformed several alternative methods, such as a low order ( $p = 1$ ) method on a strongly refined, asymptotically optimal mesh. The method has been seen to be extremely robust and efficient for arbitrarily small boundary layer widths (we tested widths down to  $O(10^{-8})$  without seeing any deterioration in the convergence rate).

In closing, we comment on the relevance of one dimensional model problems. We decoupled completely the stability analysis of the scheme from the approximability of the solution and obtained exponentially convergent boundary layer approximation in one dimension. Boundary layers in two and three dimensional problems typically show the behavior  $\exp(-x/\varepsilon)$  only in one direction, namely *normal* to the boundary or the front (see, e.g. the results for the Reissner-Mindlin plate in [1]). Therefore, using a tensor product argument, our approximation results apply directly to these situations [10], [12], [14], provided the grids are aligned with the boundary layer. For example, for the viscous flows around profiles, the current use of highly-refined, body-fitted meshes towards the profile in finite difference methods corresponds to the use of the exponential mesh in our experiments. A 2-layer mesh for the *hp* method is certainly simpler to generate, once the scale parameter  $\varepsilon$  of the layer has been estimated. The savings in the number of degrees of freedom in one dimension over the low order method with exponential mesh (45) will be increased in proportion to the number of degrees of freedom used along the boundary or the front.

The issue of an efficient numerical implementation of the unsymmetric method are, due to the implicit nature of the trial functions, to be investigated further, especially in higher dimensions.

## 7 Acknowledgements

This work was supported under AFOSR grant F49620-J-0100.

## References

- [1] D.N. Arnold and R.S. Falk, *Asymptotic analysis of the boundary layer for the Reissner-Mindlin plate model*, SIAM J. Math. Anal., 27, 1996.
- [2] I. Babuška and B.A. Szabo, *Lecture notes on finite element analysis*, to appear.
- [3] I. Babuška and W.G. Szymczak, *An error analysis for the finite element method applied to convection diffusion problems*, Comp. Meth. Appl. Mech. Engg. 31 (1982) 19-42.
- [4] I.A. Blatov and V.V. Strygin, *On estimates best possible in order in the Galerkin finite element method for singularly perturbed boundary value problems*, Russian Acad. Sci. Dokl. Math. 47 (1993), 93–96.
- [5] C. Canuto, *Spectral methods and a maximum principle*, Math. Comp. 51 (1988), 615–629.
- [6] E.C. Gartland, *Uniform high-order difference schemes for a singularly perturbed two-point boundary value problem*, Math. Comp. 48 (1987), 551–564.
- [7] W.B. Liu and J. Shen, *A new efficient spectral Galerkin method for singular perturbation problems*, Preprint, Department of Mathematics, Penn State University, State College Pa (1994).
- [8] H. Kraus, *Thin elastic shells - an introduction to the theoretical foundations and the analysis of their static and dynamic behavior*. New York, Wiley (1967).
- [9] A. Schatz and L. Wahlbin, *On the finite element method for singularly perturbed reaction-diffusion problems in two and one dimensions*, Math. Comp. (1983), 47-89.
- [10] C. Schwab and M. Suri, *Locking and boundary layer effects in the finite element approximation of the Reissner-Mindlin plate model*, Proc. Symp. Appl. Math. 48 (1994), 367–371.
- [11] C. Schwab and M. Suri, *The  $p$  and  $hp$  versions of the finite element method for problems with boundary layers*, to appear in Math. Comp.
- [12] C. Schwab, M. Suri, and C. Xenophontos, *The  $hp$  finite element method for problems in mechanics with boundary layers*, to appear.
- [13] R. Vulanović, D. Herceg and N. Petrović, *On the extrapolation for a singularly perturbed boundary value problem*, Computing 36 (1986), 69–79.
- [14] C. A. Xenophontos, *The  $hp$  version of the finite element method for singularly perturbed problems in unsmooth domains*, Ph.D. Dissertation, UMBC, to appear.